INT. J. REMOTE SENSING, 10 DECEMBER, 2004,
VOL. 25, NO. 23, 5415–5427

Taylor & Francis
Taylor & Francis Group

Effect of senescent leaves on NDVI-based estimates of *f*APAR: experimental and modelling evidences

C. M. DI BELLA †‡*, J. M. PARUELO§, J. E. BECERRA†§, C. BACOUR¶ and F. BARET¶

†Instituto de Clima y Agua, INTA, Los Reseros y Las Cabañas S/N (1712), Castelar, Buenos Aires, Argentina
‡Departamento de Producción Animal, Cátedra de Forrajes, Facultad de Agronomía, Universidad de Buenos Aires, Av. San Martín 4453, C1417DSE, Ciudad Autónoma de Buenos Aires, Argentina
§Laboratorio de Análisis Regional y Teledetección (LART), IFEVA, Cátedra de Ecología-Facultad de Agronomía, UBA Av. San Martín 4453, C1417DSE, Ciudad Autónoma de Buenos Aires, Argentina
¶INRA-CSE, Site Agroparc, Domaine Saint-Paul, 84914 Avignon Cedex 9, France

(*Received 9 October 2003; in final form 10 May 2004*)

Abstract. Spectral indices from remotely sensed data, such as the Normalized Difference Vegetation Index (NDVI), are often used to estimate biophysical characteristics of vegetation. The objective of this study is to evaluate the effect of senescent leaves on the estimation of the fraction of photosynthetically active radiation absorbed by the green elements of the canopy ($f\mathrm{APAR}_g$) from NDVI measurements. An experiment was conducted under controlled conditions over grass canopies. Both NDVI and $f\mathrm{APAR}_g$ were measured when the cover fraction by senescent leaves was changed. The results demonstrated that the effect of senescent leaves was significant on NDVI values. A similar effect was observed on the $f\mathrm{APAR}_g$ values. In these conditions, simple models were developed to relate the $f\mathrm{APAR}_g$ to NDVI values when the cover fractions of the senescent leaves vary. When combining these models, a linear relationship was found between NDVI and $f\mathrm{APAR}_g$, which was in good agreement with our experimental observations. Complementary radiative transfer model simulations were then run and confirmed these results. In addition, the vertical and horizontal distribution of the senescent leaves was investigated. They show that the relationship between NDVI and $f\mathrm{APAR}_g$ was only marginally affected by the distribution of the senescent leaves.

1. Introduction

In the last 20 years, remotely sensed data have become an important tool to study the temporal and spatial variations of structural and functional attributes of ecosystems (Davis and Roberts 2000, Running *et al.* 2000). The use of remotely sensed data in such studies is often based on the contrast observed over photosynthetic tissues in the red and infrared reflectance values. Because of

*Corresponding author; e-mail: cdibella@cnia.inta.gov.ar

International Journal of Remote Sensing
ISSN 0143-1161 print/ISSN 1366-5901 online © 2004 Taylor & Francis Ltd
http://www.tandf.co.uk/journals
DOI: 10.1080/01431160412331269724

chlorophyll absorption, green leaves reflect a small proportion of the incoming radiation in the red and a high proportion in the near infrared bands (Guyot 1990). Several indices have been generated combining information from these two bands. One of the most widely used indices is the Normalized Difference Vegetation Index (NDVI) (Rouse *et al.* 1974, Bannari *et al.* 1995) (equation (1)):

$$\mathrm{NDVI} = \frac{\mathrm{NIR} - \mathrm{R}}{\mathrm{NIR} + \mathrm{R}} \tag{1}$$

where R is the red band and NIR is the near infrared band. NDVI values range between -1 and 1. Thus high values could be associated with photosynthetic activity, due to a reduction in leaf reflectance in the red band because of chlorophyll absorption and an increase in infrared reflection due to the leaf structure (Baret 1990). Strong relationships have been reported between NDVI and some structural and functional characteristics of vegetation such as biomass (Tucker 1977a,b, Gerberman *et al.* 1984, Ripple 1985, Sellers 1985), Leaf Area Index (LAI) (Curran 1983, Asrar *et al.* 1984, Baret *et al.* 1989), Aerial Net Primary Productivity (ANPP) (Prince 1991, Paruelo *et al.* 1997) or Absorbed Photosynthetic Active Radiation (APAR) (Goward *et al.* 1994, Gamon *et al.* 1995). Such relationships lead to many applications of NDVI in regional studies, including land use and land cover classifications (Guerchman *et al.* 2003), estimates of livestock stocking density (Oesterheld *et al.* 1998) or actual evapotranspiration (Di Bella *et al.* 2000). Nevertheless, the NDVI may not be sensitive in some cases to changes in vegetation structure, i.e. LAI or biomass. Variations in soil background, atmosphere variations, leaf orientation, canopy structure, sun or viewing angle and leaf optical properties may affect the relationship between NDVI and such structural variables (Baret *et al.* 1989, Baret and Guyot 1991).

Based on theoretical considerations, Sellers (1989) demonstrated that the nature of the exponential relationship between the absorbed fraction of Photosynthetic Active Radiation (*f*APAR) and LAI is described by an extinction coefficient ($k_{f\mathrm{APAR}}$), which explains the radiation attenuation into the canopy. Similarly, NDVI is also related to LAI by an exponential relationship characterized by an extinction coefficient k_{NDVI} (Asrar *et al.* 1984). Because $k_{f\mathrm{APAR}}$ and k_{NDVI} values are similar, it follows that *f*APAR and NDVI are almost linearly correlated (Sellers *et al.* 1992). Despite the empirical and theoretical evidence supporting the use of spectral indices to estimate structural or functional variables of the canopy, some critical questions still remain unsolved. A particularly important question for grass-dominated systems is the influence of dead material on the radiative transfer in the canopy and the possible consequences on the relationship between NDVI and canopy characteristics.

Few studies have analysed the influence of standing dead biomass on canopy reflectance under experimental conditions. Asner (1998) highlighted the importance of increasing radiation transfer measurements at the canopy level. On the other hand Gamon *et al.* (1995) showed that additional estimates of dead tissue biomass, which can be dominant in certain types of vegetation, are needed to estimate canopy green biomass from NDVI values. Serrano *et al.* (2000) indicated the importance of removing non-photosynthetic materials, like dead or senescent biomass, when spectral measurements are carried out in the canopy to estimate characteristics associated with the green parts. Most of the investigations on canopy structure effects on the estimates of biomass or *f*APAR from vegetation indices are based on models and generally only green elements are taken into account.

In this article we investigated the effect of standing dead biomass on NDVI and *f*APAR using two approaches, manipulative experiment and simulation analyses using a Radiative Transfer Model (RTM). We analysed to what extent the effect of senescent leaves on NDVI is due to changes in the spectral characteristics of the whole canopy or to changes in the amount of canopy absorbed radiation by the canopy (*f*APAR).

2. Materials and methods

Two sets of experiments were conducted to study the effect of the presence of senescent leaves on the NDVI-*f*APAR relationship. The first one corresponded to actual measurements under controlled conditions. The second one consisted of simulating a range of conditions with a RTM.

2.1. *Experiments under controlled conditions*

Plants of ryegrass (*Lolium perenne L.* var. Manhattan) were cultivated in pots of 15 cm diameter and 15 cm height. Plants grew at 20–25°C during the day and 15–20°C during the night and were fertilized at tillering with urea (44 kg N ha^{-1}) to eliminate possible nitrogen deficiencies. Pots were watered to field capacity every two days, eliminating major water stress.

A basic matrix of 16 pots (4 × 4 pots) was designed to simulate the canopy (figure 1(*a*)). Above the canopy, a structure (figure 1(*c*)) bordered by a neutral filter was placed to eliminate external sources of diffuse radiation. A special wire mesh mounted on this structure (figure 1(*c*), position A) allowed strips of senescent material of ryegrass to be placed on top of the canopy. Each strip was 60 cm long × 6 cm wide and 0.3 cm deep and covered 10% of the total surface of the canopy of 60 cm × 60 cm (figure 1(*a*)). The wire mesh on which we placed the strips intercepted a small fraction of radiation (less than 3.6%).

Radiometric and photosynthetic active radiation (PAR) measurements were performed using this experimental design. A SKYE SKR100 (Skye Instruments Ltd, UK) radiometer was used to measure the R/NIR ratio (660/730 nm), from which the NDVI value was derived. A reference panel surface (Spectralon) was used every three measures to normalize for changes in illumination conditions and to obtain calibrated NDVI values. A one-metre linear sensor LICOR (Li Quantum Sensor) was used to measure PAR. Taking into account that the canopy was 60 cm wide, we covered 40 cm of the sensor with black polyethylene. All measurements were performed at noon during 1 hour under completely clear sky conditions.

Measurements of NDVI were performed with nine replicates, each one covering 1/9 of the total surface (figure 1(*b*)). Five replicates of PAR were measured at different levels (figure 1(*c*)). The fraction f of PAR absorbed by a horizontal layer above a background (f) could be expressed as:

$$f = 1 - \tau - \rho - \tau\rho_s \tag{2}$$

where ρ is the canopy hemispherical reflectance, ρ_s is the background hemispherical reflectance, and τ is the transmittance, ρ, τ and ρ_s being computed within the PAR domain. Because in the PAR domain, the leaves are absorbing most of the light, the terms $(\rho - \tau\rho_s)$ could be neglected. In these conditions, the fraction of PAR radiation absorbed by the canopy can be simply expressed as:

$$f = 1 - \tau \tag{3}$$

Applying equation (3) to our experimental set-up leads to the following

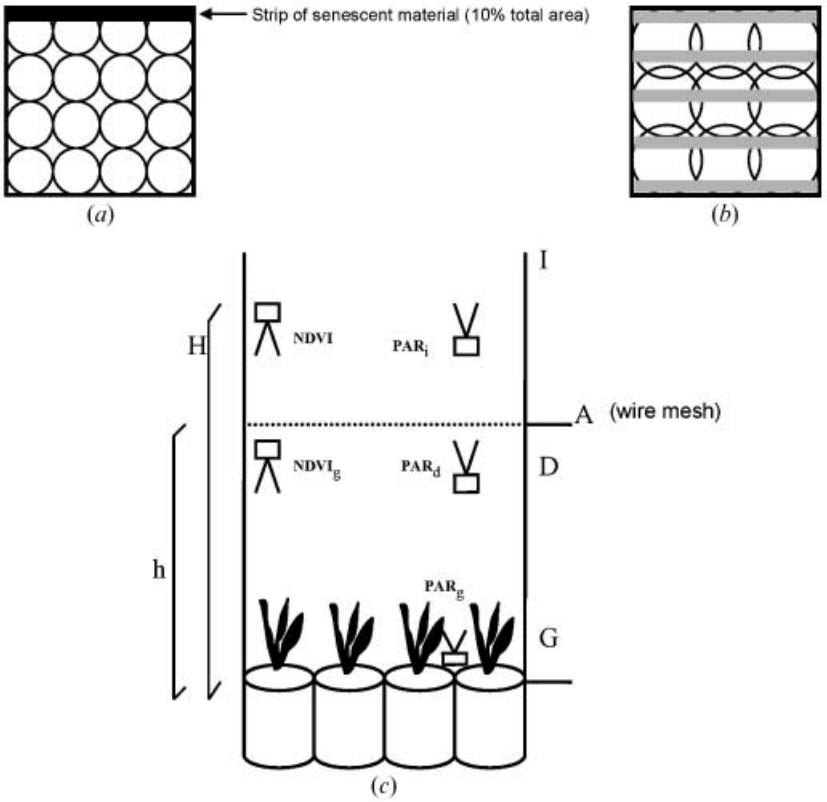

Figure 1. Controlled experiment design. (*a*) vertical view of the 4×4 pots canopy and a strip of dead biomass covering 10% of total surface; (*b*) vertical view of the nine radiometric measurements made with the radiometer (the circles represent the actual field-of-view), and the five replicates of PAR measurements (the grey rectangles); and (*c*) side view of the experimental design. The dashed line represents the level where the wire mesh tray was placed. I, D, G are measurement positions. H and h are the heights of sensor placement.

definitions of transmittances:

$$\left.\begin{aligned} \tau_t &= \frac{\mathrm{PAR}_g}{\mathrm{PAR}_i} \\ \tau_d &= \frac{\mathrm{PAR}_d}{\mathrm{PAR}_i} \\ \tau_g &= \frac{\mathrm{PAR}_g}{\mathrm{PAR}_d} \end{aligned}\right\} \tag{4}$$

where τ_t is the transmittance of the whole canopy, τ_d that of the senescent layer, and τ_g that of the green layer. PAR_i is the incoming radiation measured above the canopy (figure 1(*c*), position I), PAR_d is the PAR registered by the sensor between the strips of dead biomass and the green leaves (figure 1(*c*), position D), and PAR_g is the PAR measured by the sensor below the canopy (figure 1(*a*), position G).

The fraction of PAR absorbed by the green and dead components of the canopy (*f*APAR) was approximated by:

$$f\mathrm{APAR} = 1 - \tau_t = 1 - \tau_g \tau_d \tag{5}$$

The fraction of incoming PAR absorbed only by the green biomass ($f\mathrm{APAR}_g$) could similarly be expressed as:

$$f\mathrm{APAR}_g = (1-\tau_g)\tau_d \tag{6}$$

All the plants were harvested at the end of the experiment. The samples were dried on a stove for 48 hours (65°C) and weighed to determine dry weight.

Using this experimental design two experiments were carried out to evaluate the effect of senescent biomass:

First experiment: we generate 11 levels of senescent leaf cover, ranging from 0 up to 100%, by adding strips of senescent tissue on top of the wire mesh. Each strip placed on the structure (figure 1(*c*), position A) covered 10% (figure 1(*b*)). The position of the strips was randomly assigned.

Second experiment: we considered two factors: the cover of senescent biomass and the amount of green biomass present in the canopy. Four levels of senescent biomass were generated by placing strips on top of the wire mesh, as in the first experiment. In addition, we included 2, 4, 8 or 10 pots where the biomass was uniformly reduced by cutting the leaves to one cm height two days before the measurements. This reduction allowed us also to generate a green biomass gradient.

2.2. *Model simulation*

Simulations of NDVI and *f*APAR have been performed with the SAIL radiative transfer model (Verhoef 1984, 1985) to confront the experimental and theoretical results. In addition, the effect of the dead biomass distribution on canopy reflectance and *f*APAR will be analysed. The SAIL canopy radiative transfer model (Verhoef 1984, 1985) calculates the reflectance, transmittance and absorptance of the canopy from a limited number of variables describing its architecture and the optical properties of the soil and leaves. Thus, the following input variables are required: the LAI, the mean leaf inclination angle (ALA) assuming an ellipsoidal distribution of foliage elements (Campbell 1990), the hot spot parameter (s_l), soil reflectance and leaf optical properties. The latter are computed thanks to the PROSPECT model (Jacquemoud and Baret 1990), which simulates leaf reflectance and transmittance spectra in the optical domain, given the leaf structure parameter (N), the chlorophyll *a* and *b* contents C_{ab} ($\mu\mathrm{g\,cm^{-2}}$), the equivalent water thickness C_w (cm), the dry matter content C_m ($\mathrm{g\,cm^{-2}}$) and the brown pigment concentration (C_{bp}) (Jacquemoud and Baret 1990, Baret and Fourty 1997). Finally, the multi-layer version of SAIL used in this investigation (Weiss *et al.* 2001) allows canopies composed of foliar elements exhibiting different optical properties to be considered (green and senescent leaves in particular).

The values of the input variables were chosen to mimic the actual values observed under the natural conditions for the grass canopies considered in the three experiments. The soil reflectance corresponded to a typical dark soil with a high organic matter content. When the variables were not precisely known, typical values were selected. Table 1 shows the results. The simulations were performed from 400 to 750 nm with a 5 nm step. The *f*APAR values were computed by integrating the absorptance vertically through the canopy depth, and spectrally between 400–700 nm. Only the green elements were used in this *f*APAR computation in good agreement with the $f\mathrm{APAR}_g$ values measured in the

Table 1. Values of the PROSPECT + SAIL input variables describing the green canopy (green layer) and the mixed canopy (green layer + senescent layer). N = leaf structure parameter; C_{ab} = chlorophyll a and b content; C_m = dry matter content; C_w = equivalent water thickness; C_{bp} = brown pigment concentration; LAI = Leaf Area Index; ALA = mean leaf inclination angle; HOT = hot spot parameter.

Inputs	Variables	Green layer	Senescent layer
Leaf optical properties	N	1.3	4
	C_{ab} (μg cm^{-2})	60	0
	C_m (g cm^{-2})	0.002	0.002
	C_w (cm)	0.004	0.004
	C_{bp}	0	5
Canopy structure	LAI	4	3
	ALA	57°	0°
	HOT	0.25	0.25

experiments. It also obviously corresponds to the required quantity when using *f*APAR values within photosynthetic models. Conversely, the NDVI values were obviously computed by simulating the reflectance at 660 nm and 730 nm, accounting for the contribution of all the elements (green and senescent).

Three types of canopies were simulated (figure 2):

Canopy 1: The canopy is composed of a green leaf homogeneous layer under one incomplete layer of senescent leaves. This corresponds to the actual conditions in the controlled experimental setup. Let C be the fraction of senescent leaves, with C varying between 0 and 1.0 by 0.1 steps. The resulting canopy reflectance, ρ_T, was approximated as the weighed sum of the reflectance of the pure green layer (ρ_G) and that of the mixed canopy composed of the green layer under the complete senescent layer (ρ_{GS}):

$$\rho_T = \rho_G(1-C) + \rho_{GS}C \tag{7}$$

Similarly, absorption by the green foliar elements α_T^G of the total canopy is given by:

$$\alpha_T = \alpha_G(1-C) + \alpha_{GS}C \tag{8}$$

where α_G is the absorption by the green elements in the complete green layer and α_{GS} is that of the complete green layer under the complete senescent layer.

Canopy 2: The canopy is composed of a complete and homogeneous layer of

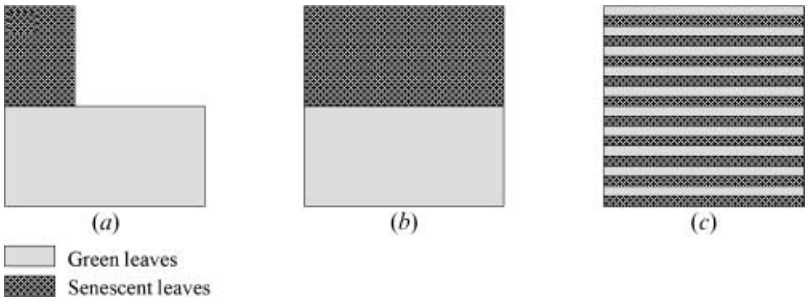

Figure 2. Scheme of the three types of canopies simulated by the radiative transfer model (RTM). (*a*) Canopy 1, (*b*) canopy 2, (*c*) canopy 3.

green leaves under a complete and homogeneous layer of senescent leaves. This situation corresponds better to actual natural conditions, although it is more difficult to simulate experimentally. The LAI of the senescent layer varied from 0 to 3 with 11 equidistributed levels.

Canopy 3: The canopy consisted of 20 layers alternatively made up of green and senescent leaves. This corresponds to the situation where the green and senescent leaves are homogeneously distributed within the canopy depth. It should be considered as a possible actual situation, and also as an intermediate between the two first situations. The total LAI for the senescent layer was similarly varied from 0 to 3 with 11 equidistributed levels. The absorption by the green elements was computed as the sum of the absorption of each 10 elementary green layers.

Except for the senescent leaf cover fraction (C) in canopy 1 and the LAI of the senescent layers for canopies 2 and 3, the other input variables remain the same (table 1).

3. Results

The NDVI measured under the senescent leaf layer ($NDVI_g$) in the first experiment remained constant (around 0.9) for all the senescent cover fractions (figure 3). In contrast, the NDVI values measured over the senescent layer decreased when the cover fraction of the senescent leaves increased (figure 3). The high variability observed for the average NDVI values was due to the location of the senescent leaf strips that were integrated in each one of the measures. It is obviously

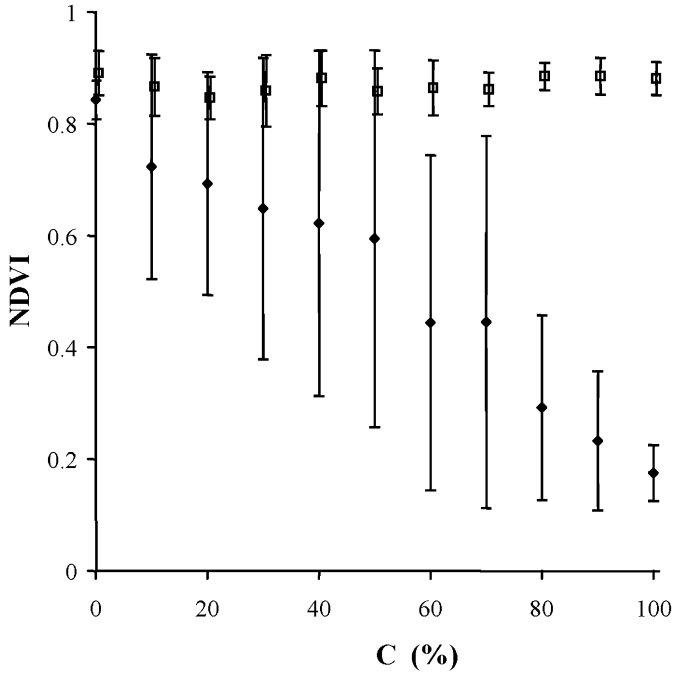

Figure 3. Relationship between the senescent cover fraction (C) and the NDVI measured at different positions: integrating the effect of senescent and green biomass over the senescent layer (NDVI ◆) and below the senescent biomass layer ($NDVI_g$ ⊟). Error bars represent ±1 SD of nine averaged measurements.

maximal for the cover fractions of the senescent leaves close to 0.5, and minimal for extreme senescent leaf cover fractions. This linear decrease of NDVI with the senescent leaf cover fraction is similar to the increase of NDVI with the vegetation fraction. This similarity is explained by the optical properties of the dead vegetation: very little transmission and a low NDVI value associated with the dead materials (in this case about $NDVI_d = 0.2$). Conversely, the full green vegetation has a NDVI value close to $NDVI_g = 0.85$. It is therefore possible to relate the NDVI value to the senescent leaf cover fraction C:

$$NDVI(C) = NDVI(1) + C(NDVI(0) - NDVI(1)) \quad (9)$$

where NDVI(0) and NDVI(1) correspond respectively to the NDVI values for a full green cover layer ($C = 0$), and to that of a complete senescent leaf layer ($C = 1$).

Incoming PAR (PAR_i) in the first experiment was approximately constant during the experiment, around $850\,\mu mol\,s^{-1}\,m^{-2}$ (figure 4) confirming the stable illumination conditions. The amount of PAR measured below the senescent leaf layer (PAR_d) decreased linearly as the senescent cover fraction increased ($r^2 = 0.99$; $n = 11$; $p < 0.001$). Note that when the senescent leaf cover fraction is complete ($C = 1$), there is still a significant level of radiation ($PAR_d(1) = 200\,\mu mol\,s^{-1}\,m^{-2}$) because of possible small gaps in the senescent leaf cover, and also because the layer is still transmitting some radiation, particularly in the longer wavelengths, where absorption by the brown pigments is weaker (figure 4). This behaviour could be simply formalized by the following equation, expressed in transmittance τ_d by

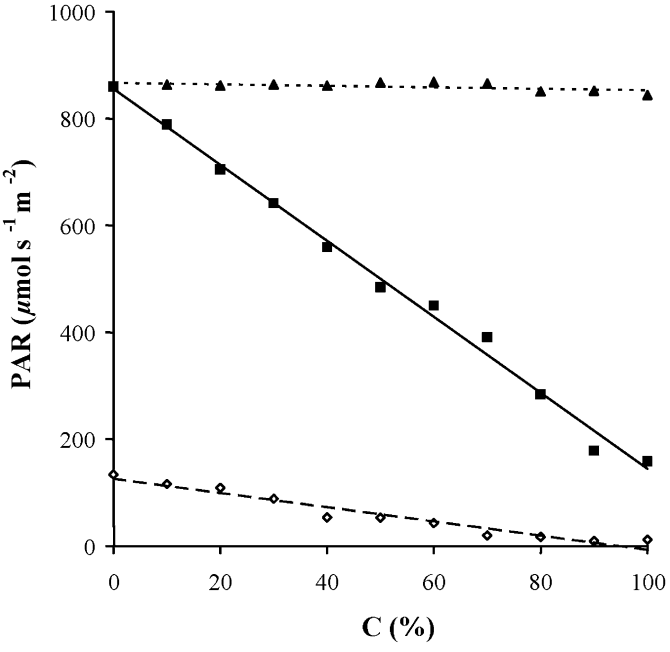

Figure 4. Relationship between senescent cover fraction (C) and PAR measured at different positions. PAR_i = above the canopy or intercepted PAR (▲); PAR_d = between the senescent and green biomass (■) and PAR_g = measurement made down the canopy (◇).

normalizing the PAR_d fluxes by the incident PAR (PAR_i):

$$\tau_d(C) = 1 - C(1 - \tau_d(1)) \tag{10}$$

Similarly, the amount of radiation measured below the green layer linearly decreases when the senescent leaf cover fraction increases, because of the reduction in the amount of incoming PAR (PAR_d) above the green layer ($r^2 = 0.94$; $n = 11$; $p < 0.001$).

Using equations (7), (8) and (10) leads to the following expressions for the fractions of PAR flux absorbed by the whole canopy (*f*APAR) and only the green layer ($f\mathrm{APAR}_g$):

$$\begin{aligned} f\mathrm{APAR}(C) &= 1 - \tau_g[1 - C(1 - \tau_d(1))] \\ &= f\mathrm{APAR}(0) - C(f\mathrm{APAR}(0) - f\mathrm{APAR}(1)) \end{aligned} \tag{11}$$

$$\begin{aligned} f\mathrm{APAR}_g(C) &= (1 - \tau_g)[1 - C(1 - \tau_d(1))] \\ &= f\mathrm{APAR}_g(0) - C\big(f\mathrm{APAR}_g(0) - f\mathrm{APAR}_g(1)\big) \end{aligned} \tag{12}$$

We observed that the relationship between *f*APAR and $f\mathrm{APAR}_g$ and the senescent leaf cover fraction is linear. By replacing the senescent leaf cover fraction C in equations (11) and (12) with its expression as a function of NDVI (equation (9)), we obtain the following expressions:

$$f\mathrm{APAR}(C) = f\mathrm{APAR}(0) - \frac{\mathrm{NDVI}(C) - \mathrm{NDVI}(1)}{\mathrm{NDVI}(0) - \mathrm{NDVI}(1)}(f\mathrm{APAR}(0) - f\mathrm{APAR}(1)) \tag{13}$$

$$f\mathrm{APAR}_g(C) = f\mathrm{APAR}_g(0) - \frac{\mathrm{NDVI}(C) - \mathrm{NDVI}(1)}{\mathrm{NDVI}(0) - \mathrm{NDVI}(1)}\big(f\mathrm{APAR}_g(0) - f\mathrm{APAR}_g(1)\big) \tag{14}$$

It shows that both fractions of absorbed PAR are linearly related to NDVI values. The total fraction of absorbed photosynthetically active radiation (*f*APAR) is negatively correlated to NDVI since $f\mathrm{APAR}(0) < f\mathrm{APAR}(1)$. Conversely, the fraction absorbed by the green layer is positively correlated with NDVI values since $f\mathrm{APAR}_g(0) > f\mathrm{APAR}_g(1)$. These theoretical results are confirmed by our experimental observations (figure 5).

In the second experiment we controlled both senescent and green material amounts by introducing strips of senescent biomass and pots with reduced green biomass into the structure. Such experimental design allowed us to evaluate the relationship between NDVI and green biomass together with changes in senescent and green biomass. We found no relationship between green biomass and NDVI ($p < 0.3$). As in the first experiment, the NDVI was highly correlated to $f\mathrm{APAR}_g$ ($r^2 = 0.78$; $n = 16$ and $p < 0.001$).

The robustness of the relationship between $f\mathrm{APAR}_g$ and NDVI was checked by comparison with our simulations for the three canopies considered. Results show a very good agreement between these simulations and the experimental values (figure 6). However, we noticed slight departures for the lower NDVI and *f*APAR values, presumably because of divergence in the optical properties of the senescent leaves when simulating both *f*APAR and NDVI.

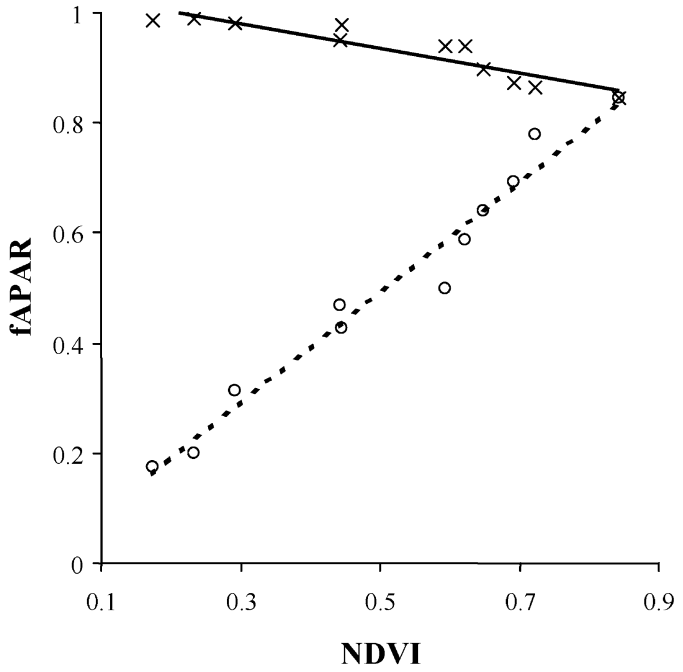

Figure 5. Fraction of PAR absorbed by the whole canopy (fAPAR, +) and by the green elements (fAPAR$_g$, o) as a function of NDVI. The lines correspond to the theoretical relationship derived from equations (13) and (14).

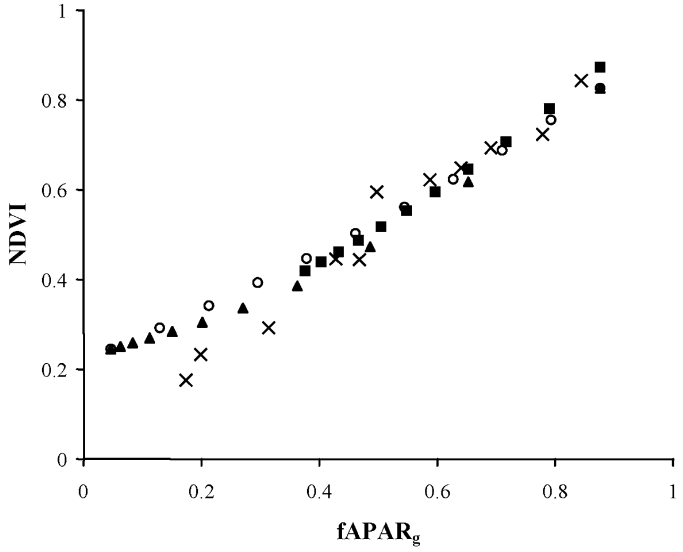

Figure 6. Relationship between the fraction of the absorbed PAR by green biomass (fAPAR$_g$) and NDVI for different conditions. (×) Measurements of first experiment (MD) (fAPAR$_g = 0.03 + 0.96$(NDVI)); (○) simulations of the first experiment (senescent leaves incomplete layer – green leaves layer (SLGL)—canopy 1) (fAPAR$_g = 0.2 + 0.7$(NDVI)); (■) multilayer simulation (ML—canopy 3) (fAPAR$_g = 0.07 + 0.9$(NDVI)); and (▲) senescent leaves – green leaves complete layer (SLVGL) simulation (canopy 2) (fAPAR$_g = 0.18 + 0.67$(NDVI)). $n = 11$, $p < 0.001$.

4. Conclusions

Our experimental results demonstrated that the effect of senescent leaves on NDVI values is significant. These results agree with Sellers (1985), van Leeuwen and Huete (1996) and Asner (1998) indicating that the presence of any significant fraction of dead material reduces vegetation indices such as NDVI. A significant effect is also observed on the fraction of photosynthetically active radiation (PAR) absorbed by the canopy. In this study, the focus was put on the absorption by the green elements which are those involved in the photosynthesis process and associated to the fraction of PAR absorbed by the green elements only ($f\mathrm{APAR}_g$). In these conditions, simple models were developed to relate $f\mathrm{APAR}_g$ to NDVI values. The experiment used mainly consisted of changing the cover fraction by senescent leaves over a complete green canopy. It shows a strong linear correlation between $f\mathrm{APAR}_g$ and NDVI as expected from the simple models extracted from the relationship between the cover fraction of senescent leaves and both $f\mathrm{APAR}_g$ and NDVI. Radiative transfer model simulations were then run to confirm these results. In addition, the vertical and horizontal distributions of the senescent leaves were manipulated and affect only marginally the relationship between NDVI and $f\mathrm{APAR}_g$.

In this study, the green and senescent leaf area index was varied trying to simulate realistic conditions. However, further work is needed to investigate a concurrent change in vertical and horizontal distributions that could be encountered over the Earth's surface.

NDVI does not provide a reliable estimate of biomass or LAI. On the contrary its linear relationship with $f\mathrm{APAR}_g$ strongly supports the use of this index to estimate primary production. Monteith's (1981) model provides the conceptual framework to integrate the spectral index device from the remote sensor into carbon gains estimations.

Acknowledgments

Paola Moglia, Gervasio Piñeiro, Rodolfo Golluscio, Gonzalo Irisarri and Gabriel Kadarián helped during data collection.This work was supported by CONICET, UBA and INTA, FONCYT (PICT99-06761) and project IICA-BID FONTAGRO/RF-01-03-RG.

References

ASNER, G. P., 1998, Biophysical and biochemical sources of variability in canopy reflectance. *Remote Sensing of Environment*, **64**, 234–253.

ASRAR, G., FUCHS, M., KANEMASU, E.T., and HATFIELD, J. L., 1984, Estimation absorbed photosynthetic radiation and leaf area index from spectral reflectance in wheat. *Agronomy Journal*, **76**, 300–306.

BANNARI, A., MORIN, D., and BONN, F., 1995, A review of vegetation indices. *Remote Sensing of Environment*, **13**, 95–120.

BARET, F., 1990, Factors and mechanisms governing canopy spectral reflectance: application for agriculture. Technical Note (Avignon: INRA).

BARET, F., and FOURTY, T., 1997, Radiometric estimates of nitrogen status in leaves and canopies. In *Diagnosis of the Nitrogen Status in Crops*, edited by G. Lemaire (Berlin: Springer), pp. 201–227.

BARET, F., and GUYOT, G., 1991, Potentials and limits of vegetation indices for LAI and APAR assessment. *Remote Sensing of Environment*, **35**, 161–173.

BARET, F., GUYOT, G., and MAJOR, D. J., 1989, Crop biomass evaluation using radiometric measurements. *Photogrammetria*, **43**, 241–256.

CAMPBELL, G. S., 1990, Derivation of an angle density function for canopies with ellipsoidal leaf angle distribution. *Agricultural and Forest Meteorology*, **49**, 173–176.

CURRAN, P. J., 1983, Multispectral remote sensing for the estimation of green leaf area index. *Philosophical Transactions of the Royal Society of London A*, **309**, 257–270.

DAVIS, F. W., and ROBERTS, D., 2000, Stand structure in terrestrial ecosystems. In *Methods in Ecosystem Science*, edited by O. E. Sala, R. B. Jackson, H. A. Mooney and R. W. Howard (Berlin: Springer), part 1 (4), pp. 7–30.

DI BELLA, C. M., REBELLA, C. M., and PARUELO, J. M., 2000, Evapotranspiration estimates using NOAA AVHRR imagery in the Pampa region of Argentina. *International Journal of Remote Sensing*, **21**, 791–797.

GAMON, J. A., FIELD, C. B., GOULDEN, M. L., GRIFFIN, K. L., HARTLEY, A. E., JOEL, G., PANUELAS, J., and VALENTINI, R., 1995, Relationships between NDVI, canopy structure, and photosynthesis, in three Californian vegetation types. *Ecological Applications*, **5**, 28–41.

GERBERMAN, A. J., CUELLAR, J. A., and GAUSMAN, H. W., 1984, Relationship of sorghum canopy variables to reflected infrared radiation for 2 wavelengths and 2 wavebands. *Photogrammetric Engineering and Remote Sensing*, **50**, 209–214.

GOWARD, S. N., WARING, R. H., DYE, D. G., and YANG, J., 1994, Ecological remote sensing at OTTER: satellite macroscale observations. *Ecological Applications*, **4**, 322–343.

GUERSCHMAN, J. P., PARUELO, J. M., DI BELLA, C. M., GIALLORENZI, M.C., and PACIN, F., 2003, Land cover classification in Argentine Pampas using multitemporal Landsat TM data. *International Journal of Remote Sensing*, **24**, 3381–3402.

GUYOT, G., 1990, Optical properties of vegetation canopies. In *Applications of Remote Sensing in Agriculture*, edited by M. Steven and J. Clark (London: Butterworths), pp. 19–43.

JACQUEMOUD, S., and BARET, F., 1990, PROSPECT: a model of leaf optical properties spectra. *Remote Sensing of Environment*, **34**, 75–91.

MONTEITH, J. L., 1981, Climatic variation and the growth of crops. *Quarterly Journal of the Royal Meteorological Society*, **107**, 749–774.

OESTERHELD, M., DI BELLA, C. M., and KERDILES, H., 1998, Relation between NOAA-AVHRR satellite data and stocking rate in grasslands. *Ecological Applications*, **8**, 206–212.

PARUELO, J. M., EPSTEIN, H. E., LAUENROTH, W. K., and BURKE, I. C., 1997, ANPP estimates from NDVI for the central grassland region of the US. *Ecology*, **78**, 953–958.

PRINCE, S. D., 1991, A model of regional primary production for use with coarse resolution satellite data. *International Journal of Remote Sensing*, **12**, 1313–1330.

RIPPLE, W. J., 1985, Asymptotic reflectance characteristics of grass vegetation. *Photogrammetric Engineering and Remote Sensing*, **43**, 1915–1921.

ROUSE, J. W., HAAS, R. H., SCHELL, J. A., and DEERING, D. W., 1974, Monitoring vegetation systems in the Great Plains with ERTS. *Proceedings of the Third Earth Resources Technology Satellite-1 Symposium* (Greenbelt: NASA), SP-351, pp. 301–317.

RUNNING, S. W., THORNTON, P. E., NEMANI, R., and GLASSY, J. M., 2000, Global terrestrial gross and net primary productivity from the Earth observing system. In *Methods in Ecosystem Science*, edited by O. E. Sala, R. B. Jackson, H. A. Mooney and R. W. Howard (Berlin: Springer), part 1 (4), pp. 44–57.

SELLERS, P. J., 1985, Canopy reflectance, photosynthesis, and transpiration. *International Journal of Remote Sensing*, **8**, 1335–1372.

SELLERS, P. J., 1989, Theory and applications of optical remote sensing. In *Vegetation—Canopy spectral reflectance and biophysical processes*, edited by G. Asrar (New York: John Wiley and Sons), pp. 297–333.

SELLERS, P. J., BERRY, J. A., COLLATZ, G. J., FIELD, C. B., and HALL, F. G., 1992, Canopy reflectance, photosynthesis, and transpiration. III. A reanalysis using improved leaf models and a new canopy integration scheme. *Remote Sensing of Environment*, **42**, 187–216.

SERRANO, L., GAMON, J. A., and PAÑUELAS, J., 2000, Estimation of canopy photosynthetic and non-photosynthetic components from spectral transmittance. *Ecology*, **81**, 3149–3162.

TUCKER, C. J., 1977a, Resolution of grass canopy biomass classes. *Photogrammetric Engineering and Remote Sensing*, **43**, 1050–1067.

TUCKER, C. J., 1977b, Asymptotic nature of grass canopy spectral reflectance. *Applied Optics*, **16**, 1151–1157.

VAN LEEUWEN, W. J. D., and HUETE, A. R., 1996, Effects of standing litter on the biophysical interpretation of plant canopies with spectral indices. *Remote Sensing of Environment*, **55**, 123–138.

VERHOEF, W., 1984, Light scattering by leaf layers with application to canopy reflectance modeling: the SAIL model. *Remote Sensing of Environment*, **16**, 125–141.

VERHOEF, W., 1985, Earth observation modelling based on layer scattering matrices. *Remote Sensing of Environment*, **17**, 165–178.

WEISS, M., TROUFLEAU, D., BARET, F., CHAUKI, H., PREVOT, L., OLIOSO, A., BRUGUIER, N., and BRISSON, N., 2001, Coupling canopy functioning and radiative transfer models for remote sensing data assimilation. *Agricultural and Forest Meteorology*, **108**, 113–128.